AN EFFICIENT NUMERICAL METHOD FOR DETERMINATION OF SHAPES, SIZES AND ORIENTATIONS OF FLAWS FOR NONDESTRUCTIVE EVALUATION

Y. M. Chen and S. L. Wang

Department of Applied Mathematics and Statistics
State University of New York at Stony Brook
Stony Brook, New York 11794, U.S.A.

INTRODUCTION

The generalized pulse-spectrum technique (GPST)[1] is a versatile and effcient iterative numerical algorithm for solving inverse problems (to determine the unknown coefficients, initial-boundary values, sources, and geometries of the space domain from the additionally measured data in the space-time domain or the space-complex frequency domain) of a system of nonlinear partial differential equations. Mathematically, inverse problems of partial differential equations can be formulated as ill-posed nonlinear operator equations. It is important to point out that the GPST is not a single narrowly defined iterative numerical algorithm but a broad class of iterative numerical algorithms based on the concept that either the nonlinear operator equation is first linearized by any one of the Newton-like iteration methods and then each iterate is solved by using a stabilizing method, e.g., the Tikhonov's regularization method[2], or the stabilizing method is first applied to the nonlinear operator equation and then the regularized nonlinear problem is solved by using a Newton-like iteration method. Hence different choices of various Newton-like iteration methods and stabilizing methods lead to different special forms of GPST, and the efficiency of GPST will then depend upon the particular choices of them and how efficiently one can treat every minute step in the numerical algorithm.

The capability of GPST for simultaneous determination of bulk modulus, shear modulus and density variation of an inhomogeneous elastic solid in nondestructive evaluation and geophysical prospecting has been demonstrated elsewhere.[1,3,4] However, if only the shapes, sizes and orientations of flaws are of interest, the efficiency of GPST can be greatly improved by choosing a special form of GPST dedicated to these types of inverse problems. This special version of GPST is versatile enough that the measurement data (both incident and scattered waves) can be the near fields, the intermediate fields, as well as the far fields. For simplicity, only inverse scattering problems for time-harmonic acoustic wave (data measured in the space-complex frequency domain) are considered. A comprehensive survey of other methods for solving inverse scattering problems for time-harmonic acoustic waves can be found in the article by Colton.[5] Moreover, for economic reasons, numerical simulations are car-

ried out only for the two-dimensional inverse problems without real measurement data to test the feasibility and to study the intrinsic characteristics of GPST. Finally, the numerical results are discussed and it is found that this GPST fares very well with regard to the following four practical criteria for the evaluation of any numerical method:

(a) Universality criterion: Can a numerical method which is effective in one-space-dimensional problems be extended with similar success into higher-space dimensional applications? Can a solution method which is effective for solving inverse problems of one type of equations, e.g., hyperbolic or parabolic type, be extended to solve the inverse problems of the other type of partial differential equations with similar success and minimum efforts?

(b) Economy of data acquisition criterion: The numerical method should be able to keep the difficulties and the cost expenditure of acquiring or measuring the necessary data for a successful calculation to a minimum.

(c) Economy of programming effort criterion: The numerical method should be as close to the nondedicated program as possible, for existing practices of programming new dedicated numerical methods for every special types of problems can be unacceptably costly in many practical circumstances. Furthermore, the computer code should also contain as many as possible of the modules where the canned subroutines can be readily called upon.

(d) Economy of computing cost criterion: The numerical method should keep the cost of IO and CPU times and memory storage to minimum.

NUMERICAL ALGORITHM

Consider the following exterior boundary value problem of the helmholtz equation in the spherical coordinate system, $\underline{R} \equiv (r,\theta,\phi)$,

$$r^{-2}\cdot\partial(r^2\partial u(\underline{R})/\partial r)/\partial r + (r^2\sin\theta)^{-1}\,\partial(\sin\theta\cdot\partial u(\underline{R})/\partial\theta)/\partial\theta + (r^2\sin\theta)^{-1}\,\partial^2 u(\underline{R})/\partial\phi^2 + k^2 u(\underline{R}) = f(\underline{R}), \quad \underline{R} \in E^3 - D, \tag{1}$$

$$u(\underline{R}) = 0, \quad \underline{R} \in S \equiv R(\theta,\phi), \tag{2}$$

and the radiation condition, $$\lim_{r\to\infty} r(\partial/\partial r - ik)u(\underline{R}) = 0, \tag{3}$$

where E^3 is the three-dimensional Euclidean physical space, D is a star-shaped finite sub-domain in E^3, S is the boundary of D, and $\underline{R} = 0$ is located in D (Fig. 1).

The inverse scattering problem considered here is to determine the boundary S (or D) such that u satisfies Eqs.(1)-(3) and the additionally measured data

$$u(\underline{R}) = h(\underline{R}), \quad \underline{R} \in D_s \subset E^3 - D, \text{ (Fig. 1)}. \tag{4}$$

Since it is very difficult to implement the radiation condition (3), the approximate radiation condition of Bayliss, Gunzburger and Turkel[6],

$$\partial u/\partial r + (2r)^{-1}u - iku = 0, \quad \underline{R} \in S_\infty, \text{ (Fig. 1)}, \tag{5}$$

is used at finite but large $\underline{R}$.

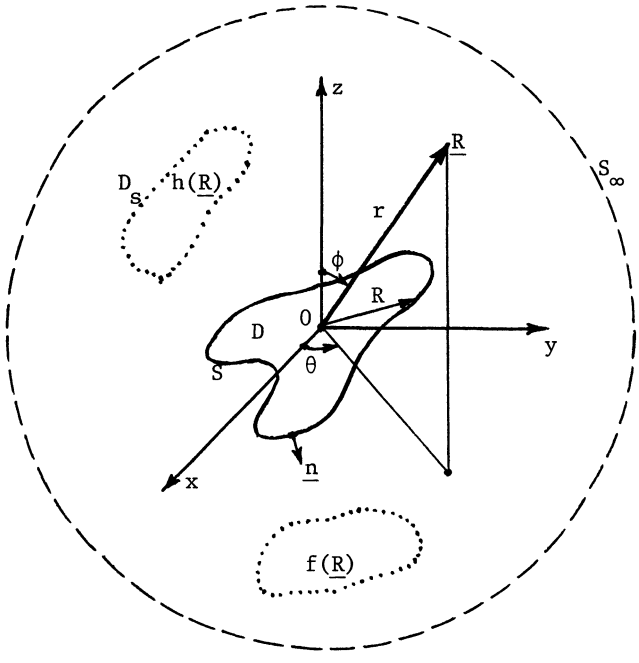

Fig. 1. The geometry of the inverse scattering problem is shown.

This GPST iterative numerical algorithm begins by setting

$$R_{n+1} = R_n + \delta R_n, \quad u_{n+1} = u_n + \delta u_n, \quad n = 0,1,2,3,\ldots\ldots, \tag{6}$$

where $R_0(\theta,\phi)$ is the initial guess for S, u_0 is the corresponding solution of (1), (2) and (5), and for numerical convergence, $|\delta R_n| < |R_n|$ and $|\delta u_n| < |u_n|$.
Upon substituting (6) into (1), (2) and (5) and neglecting terms of $O(\delta^2)$ and higher, one obtains

$$(\nabla^2 + k^2)\, u_n = f(\underline{R}), \quad \underline{R} \in E^3 - D, \tag{7}$$

$$u_n(\underline{R}) = 0, \quad \underline{R} \in R_n, \tag{8}$$

$$\partial u_n/\partial r + (2r)^{-1} u_n - iku_n = 0, \quad \underline{R} \in S_\infty, \tag{9}$$

and

$$(\nabla^2 + k^2)\, \delta u_n = 0, \quad \underline{R} \in E^3 - D, \tag{10}$$

$$\delta u_n = -(\partial u_n/\partial r)\, \delta R_n, \quad \underline{R} \in R_n, \tag{11}$$

$$\partial \delta u_n/\partial r + (2r)^{-1} \delta u_n - ik\delta u_n = 0, \quad \underline{R} \in S_\infty. \tag{12}$$

By using the method of Green's function, setting $\underline{R} \in D_s$ and hence replacing u_{n+1} by $h(\underline{R})$, one obtains a Fredholm integral equation of the first kind from (10)-(12) for δR_n,

$$\int_{S_n \equiv R_n} \partial u_n/\partial r' \cdot \partial G_n(\underline{R},\underline{R}')/\partial \underline{n}' \cdot \delta R_n(\theta',\phi')\, ds' = h(\underline{R}) - u_n(\underline{R}), \quad \underline{R} \in D_s, \tag{13}$$

where $G_n(\underline{R},\underline{R}')$ is the Green's function of Eqs.(7)-(9) and $\underline{n}_n$ is the unit normal vector outward from S_n.

Equations (6)-(9) and (13) form the basic structure for each iteration of this GPST. Boundary value problem (7)-(9) and its Green's function can be solved numerically by using the 9-point finite difference method[7]. The Fredholm integral equation of the first kind (13) is first discretized by using the trapezoidal rule and then solved by using the Tikhonov's regularization method.

NUMERICAL SIMULATION

In order to test the feasibility and to study the general characteristics of this GPST computational algorithm without the real measurement data, for economic reasons, only two-dimensional examples or three-dimensional examples with axial symmetry are used in the numerical simulation.

First, one chooses a S* which is supposed to represent the correct shape of the scatterer and a source $f(\underline{R})$. Then the boundary value problem (1), (2) and (5) is solved numerically to obtain the additionally measured data $h(\underline{R})$ for $\underline{R} \in D_s$. Next, S_0 or R_0 is assumed. Upon solving (6)-(9) and (13) numerically, R_1 is obtained. Then in a similar manner R_2 is obtained. One continues this procedure until finally a numerical limit R_N is reached. Other than the truncation and round-off errors in both generating the numerical data and computing R_N, any norm of $S^* - R_N$ can be used as a criterion for evaluating the performance of the computational algorithm of GPST. Although one can give a crude estimation of these errors, they can be considered as some kind of computer-generated errors in the numerical simulation.

In the numerical simulation, the computational grid system fits into the polar coordinates in a natural manner. However, it is divided into two regions, a core region consisting of adaptive grids which is surrounded by a region consisting of fixed grids (Fig. 2). These adaptive grids

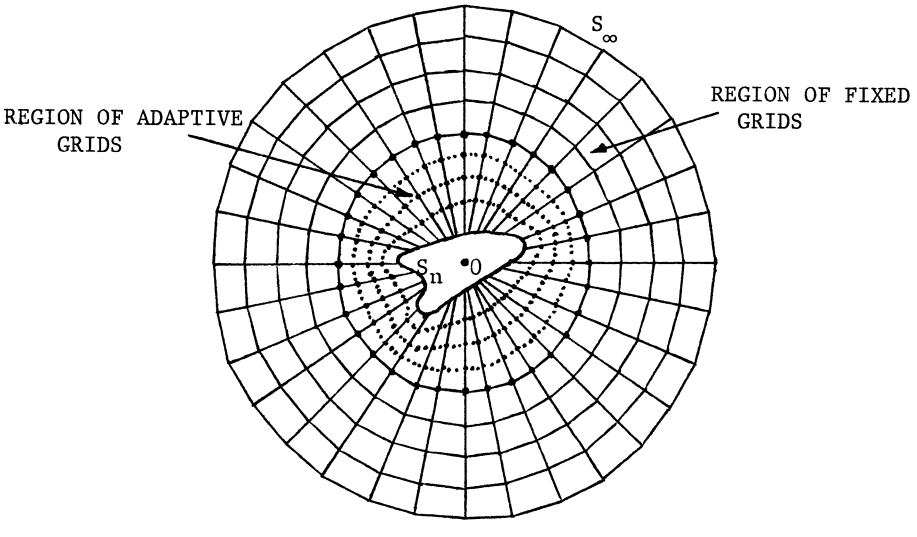

Fig. 2. The computational grid system used here.

provide a body-fitted computational grid system so that higher accuracy can be achieved with smaller number of grid points.

The numerical simulation here is carried out for (a) a large class of S* or R*, (b) k ranging from 0.01 to 2, (c) various D_s, (d) multiple incident waves from point sources at different locations, and (e) measured data contain no noise or a small amount of noise. Here only few more demanding examples are shown in Figs. 3 - 7.

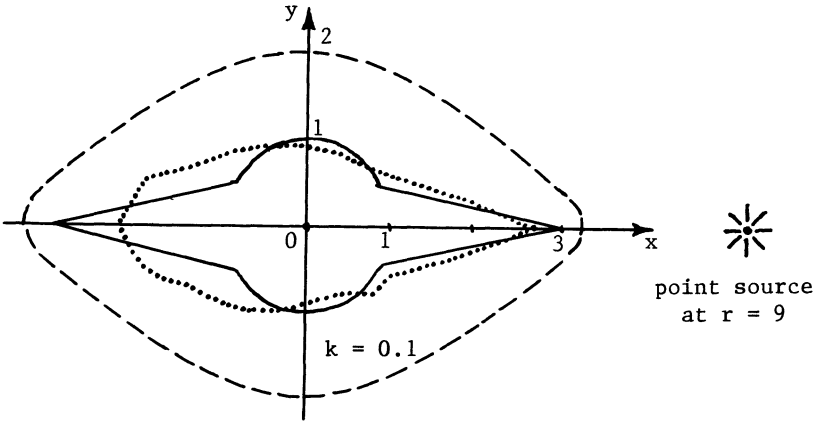

Fig. 3. Comparison of the calculated S_5..... and the exact S* ——— with the initial guess S_0-----. Data measured at every 15^o angle around the object without noise.

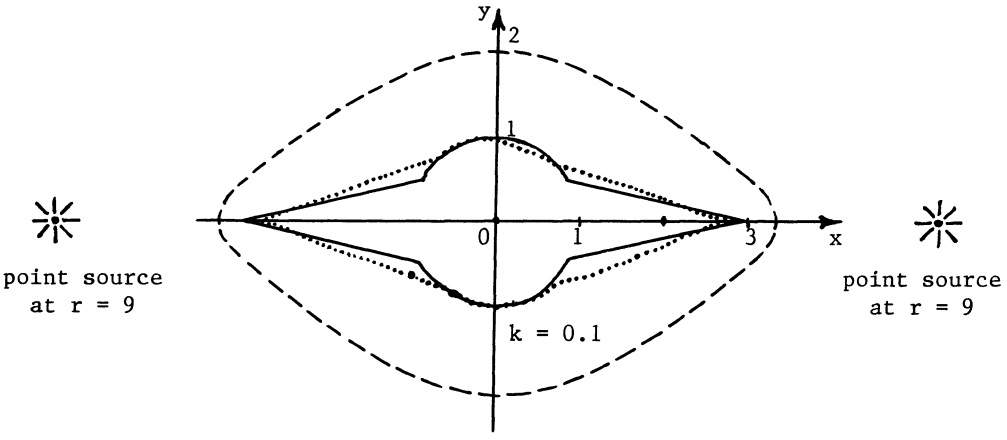

Fig. 4. Comparison of the calculated S_5..... and the exact S*——— with the initial guess S_0-----. Data measured at every 15^o angle around the object without noise.

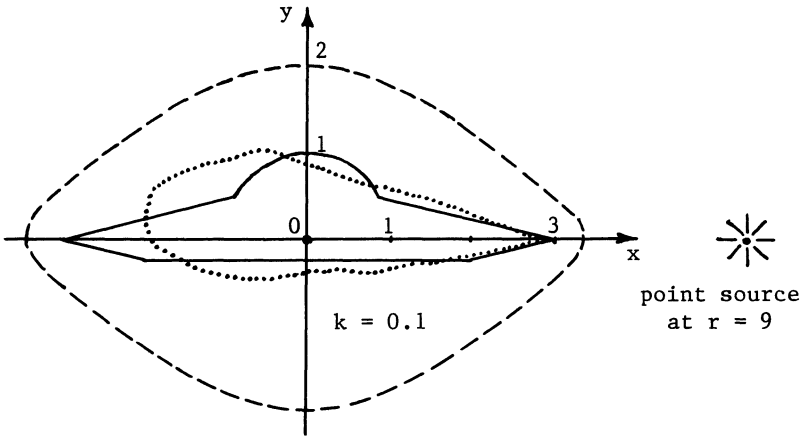

Fig. 5. Comparison of the calculated S_5..... and the exact S*——— with the initial guess S_0-----. Data measured at every 15° angle around the object without noise.

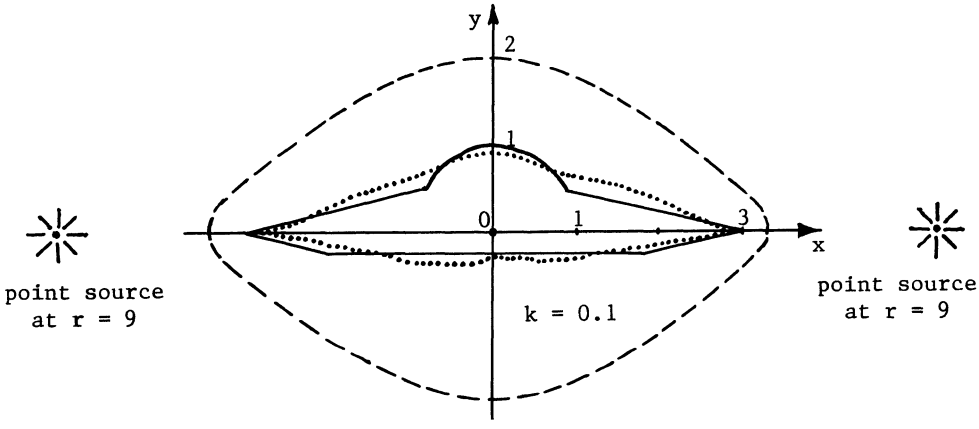

Fig. 6. Comparison of the calculated S_5..... and the exact S*——— with the initial guess S_0-----. Data measured at every 15° angle around the object without noise.

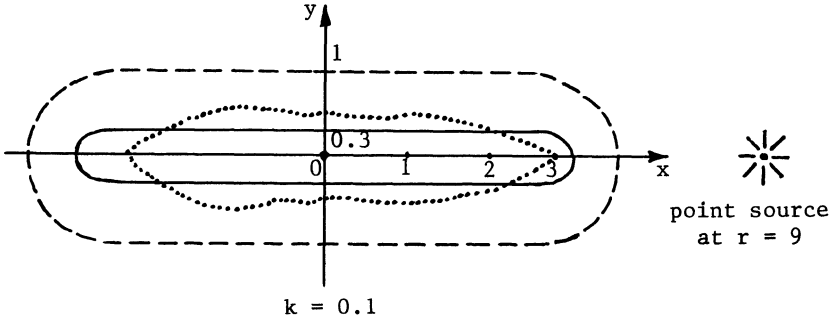

Fig. 7. Comparison of the calculated S_5..... and the exact S*——— with the initial guess S_0-----. Data measured at every 15° angle around the object without noise.

DISCUSSION

The results in the numerical simulations have demonstrated that in most situations this GPST iterative numerical algorithm does give excellent performance in determining the shapes, sizes and orientations of flaws with difficult geometries, e.g., slender bodies, winged cavities, etc. It is effective in the range $0.05 \leq kL \leq 1.00$, L being the typical size of the flaw, whereas the numerical results lack fine resolution for $kL < 0.05$ and contain large errors in the shadow region for $kL > 1.00$. The choices of different D_s and multiple incident waves does influence the numerical results. For examples, from Figs. 3 - 7 the accuracy of the numerical results in the shadow region of a single point source is relatively poor. Moreover, for cases of simpler flaws, this GPST algorithm is stable when the measured data contain random noise up to at least 5%.

Finally, it is found that this GPST is more efficient than the analytic-continuation method[8] and the Newton-Kantorovitch algorithm[9], because for this GPST the CPU time of a typical example is approximately 15 sec. on UNIVAC 1100 which is 1/2 of that for the analytic-continuation method and 1/3 of that for the Newton-Kantorovitch algorithm. Of course, the efficiency of GPST can be much more improved, if many existing and new (to be developed) ideas in numerical computation are adopted.

REFERENCES

1. Y. M. Chen, "Generalized pulse-spectrum technique (GPST) for solving problems in parameter identification," Proc. China-US Workshop on Advances in Computational Engineering Mechanics, Dalian, China, Sept. 5-9 (1983).
2. A. N. Tikhonov and V. Arsenin, "Solutions of Ill-Posed Problems," Wiley, New York (1977).
3. Y. M. Chen and G. Q. Xie, "A numerical method for simultaneous determination of bulk modulus, shear modulus and density variations for nondestructive evaluation," Nondestructive Testing Communications, (1984).
4. Y. M. Chen and G. Q. Xie, "An iterative method for simultaneous determination of bulk and shear moduli and density variations," submitted to J. Comp. Phys.
5. D. Colton, "The inverse scattering Problem for time-harmonic acoustic waves," SIAM Rev., 26:323 (1984).
6. A. Bayliss, M. Gunzburger and E. Turkel, "Boundary conditions for the numerical solution of elliptic equations in exterior regions," SIAM J. Appl. Math., 42:707 (1982).
7. Y. M. Chen and J. Q. Liu, "A numerical algorithm for solving inverse problems of two-dimensional wave equations," J. Comp. Phys., 50:193 (1983).
8. W. A. Imbriale and R. Mittra, "The two-dimensional inverse scattering problem," IEEE Trans. Ant. & Prop., AP-18:633 (1970).
9. A. Roger, "Newton-Kantorovitch algorithm applied to an electromagnetic inverse problem," IEEE Trans. Ant. and Prop., AP-29:232 (1981).